DMD Fast Forward. Published on June 21, 2006 as doi:10.1124/dmd.106.010140

DMD #10140

Title Page:

CHARACTERIZATION OF RAT INTESTINAL MICROSOMAL UDP-GLUCURONOSYLTRANSFERASE ACTIVITY TOWARDS MYCOPHENOLIC ACID

Kristini K. Miles, Fay K. Kessler, Philip C. Smith, and Joseph K. Ritter

Department of Pharmacology and Toxicology, School of Medicine, Virginia Commonwealth University, Richmond, VA (K.M., F.K. and J.R.); and Division of Molecular Pharmaceutics, School of Pharmacy, University of North Carolina, Chapel Hill, NC (P.S.), USA

RUNNING TITLE PAGE

Running title: Glucuronidation of mycophenolic acid by rat intestine

Corresponding author:
Joseph K. Ritter, Ph.D.
Dept. of Pharmacology and Toxicology
Virginia Commonwealth University
1217 E. Marshall Street, Medical Sciences Bldg. Room 531
Box 980613
Richmond, VA 23298-0613
Telephone: 804-828-1022
Fax: 804-828-0676
Email: jkritter@vcu.edu

Number of text pages: 38
Number of tables: 2
Number of figures: 7
Number of references: 27
Number of words in the Abstract: 238
Number of words in the Introduction: 586
Number of words in the Discussion: 1456

Abbreviations

EDTA	Ethylenediamine tetraacetic acid
HPLC	High performance liquid chromatography
MPA	Mycophenolic acid
MPAG	Mycophenolic acid 7-O-glucuronide
PMSF	Phenylmethylsulfonylfluoride
UDP	Uridine 5´-diphosphate
UGT	Uridine 5´-diphosphoglucuronosyltransferase

Abstract

Mycophenolic acid (MPA) is the active immunosuppressive metabolite of the anti-organ rejection drug, mycophenolate mofetil (MMF) and is implicated in the gastrointestinal toxicity associated with MMF therapy. Intestinal UDP-glucuronosyltransferases (UGTs) have been proposed to provide intrinsic resistance against MMF-induced gastrointestinal toxicity by converting MPA to the inactive MPA 7-O-glucuronide. Using an optimized intestinal microsome preparation method that stabilized the intestinal MPA UGT activity, the MPA UGT activity of male Sprague-Dawley rat intestinal microsomes was characterized. A longitudinal gradient similar to that described for other phenolic compounds was observed, with the activity decreasing from the duodenum to the distal small intestine and colon. The catalytic efficiency of MPA glucuronidation decreased from the proximal to distal intestine as a result of decreasing V_{max} and increasing K_m. The finding that homozygous Gunn rats lack detectable intestinal MPA UGT activity indicates exclusive roles of UGT1A1, UGT1A6, and/or UGT1A7. Quantitative immunoblotting revealed a parallel between the MPA UGT activity and the content of UGT1A7-like immunoreactivity (18.7 to 7.3 μg/mg for duodenum and colon, respectively). In contrast, the lesser MPA-metabolizing UGTs, UGT1A1 and UGT1A6, were lower in abundance (1.6-2.1 and 1.7-2.9 μg/mg, respectively), and their patterns of longitudinal distribution were distinct from the MPA UGT activity. These data suggest a dominant role of a UGT1A7-like enzyme, presumably UGT1A7 itself, in the catalysis of rat intestinal MPA glucuronidation. Studies are ongoing to investigate the relationship between intestinal UGT1A enzymes and susceptibility to MMF-induced gastrointestinal toxicity.

Introduction

Conjugation with glucuronic acid represents one of the most important types of phase II drug biotransformation reactions (Dutton, 1980). The enzymes catalyzing this process are the UDP-glucuronosyltransferases (UGTs) which consist of two multi-membered families of UGTs, UGT1 and UGT2 (Ritter, 2000). While the liver and kidney are commonly viewed as the major sites of glucuronidation in the body, the intestine has also received considerable attention, with microsomal UGT activities approaching or exceeding the activity values for liver (for recent reviews, see Fisher *et al.*, 2001; Tukey and Strassburg, 2001; Gregory *et al.*, 2004). Intestinal UGT activity is likely to contribute to the exclusionary function of the gastrointestinal barrier, allowing the passage of nutrients while excluding other xenobiotics present in foods. For certain drugs taken orally, intestinal UGTs are also proposed to play a role in presystemic, "first pass" drug elimination. Because glucuronide conjugates are usually less active toxicologically, they may also serve to protect the gastrointestinal mucosa from cytotoxic effects of ingested drugs and food substances.

Mycophenolate mofetil (CellCept®) is the prodrug form of MPA ((1,3-dihydro-4-hydroxy-6-methoxy-7-methyl-3-oxo-5-isobenzylfuranyl)-4-methyl-4-hexenoate), an immunosuppressive agent widely used in transplant patients to prevent graft rejection. Use of the standard initial dose of MMF in transplant patients (1 g/ bid) is associated with a high incidence of gastrointestinal toxicity (constipation and diarrhea with nausea and vomiting). The occurrence of the latter often necessitates dosage reduction, a consequence of which is reduced immunosuppressive efficacy (Busca *et al.*, 2001). MPA is excreted primarily in the urine as its inactive 7-O-phenolic glucuronide, MPAG

(Bullingham *et al.*, 1998). MPAG also undergoes biliary excretion resulting in substantial enterohepatic cycling. The observation by multiple laboratories that intestinal microsome preparations are able to efficiently glucuronidate MPA (Bowalgaha and Miners, 2001; Shipkova *et al.*, 2001; Bernard and Guillemette, 2004; Picard *et al.*, 2005) raises the question of whether interindividual differences in intestinal MPA glucuronidation influence the onset or severity of MPA-induced gastrointestinal toxicity.

Establishment of a laboratory animal model for MPA intestinal toxicity would be a valuable step taken toward testing this hypothesis. The potential utility of the rodent model is supported by the observation that male Sprague-Dawley rats treated subchronically with mycophenolate mofetil (doses > 75 mg/kg/day for 3-6 days) develop diarrhea and pathologic signs of gastrointestinal toxicity (Stern, S. and Smith, P., unpublished data). Although there are no published reports to our knowledge demonstrating activity of rat intestine in MPA glucuronidation, the rat intestine has been reported to be highly active in the glucuronidation of a number of phenolic substrates (Hietanen *et al.*, 1972; Hietanen and Vainio, 1973; Koster *et al.*, 1985; Vargas and Franklin, 1997). A recent study by our laboratory revealed significant activities (>1 nmol/mg/min) of three rat recombinant UGT1A isoforms, UGT1A1, UGT1A6, and UGT1A7 towards MPA, and each of these are expressed at significant levels in rat intestine (Kobayashi *et al.*, 1998; Grams *et al.*, 2000; Shelby *et al.*, 2003; Webb *et al.*, 2005a).

The major objective of this study was to demonstrate and characterize the microsomal MPA glucuronidating activities of rat small intestine and colon and to relate these activities to the levels of UGT1A1, 1A6, and 1A7-like protein found in these

tissues. A secondary objective was to determine the absolute contents of these UGTs in liver, kidney, and intestine microsomes through quantitative immunoblotting. Our study revealed a gradient of MPA UGT activity along the longitudinal axis of the rat intestine along with enzyme-specific patterns of expression. The marked proximal to distal gradient in MPA UGT activity was strongly correlated with the content of UGT1A7-like immunoreactivity.

Materials and Methods

Chemicals and Reagents. MPA, chymostatin (cat. # C-7268), leupeptin (L-2023), aprotinin (A-1153), antipain (A-6191), pepstatin A (P-5318), phenylmethylsulfonyl fluoride (PMSF), and soybean trypsin inhibitor (T-2011) were from Sigma Chemical (St. Louis, MO). Mycophenolate 7-O-glucuronide (MPAG) was from a preparation previously synthesized and described (Wiwattanawongsa *et al.*, 2001). Solvents used for HPLC analysis were purchased from Fisher Scientific (New Lawn, NJ). All other chemicals used were purchased from Sigma and were the highest grade available. Generation and amplification of recombinant adenoviruses coding for rat UGTs 1A1, 1A6, or 1A7 under the control of cytomegalovirus promoter sequences were previously described (Miles *et al.*, 2005).

Animals. Young adult male rats (6-8 weeks, 180-240 g body weight) were used for our studies. Sprague Dawley rats were from Harlan Sprague-Dawley (Frederick, MD). Homozygous j/j rats or heterozygous j/+ Gunn rats were from a breeding colony established at Virginia Commonwealth University. Animals were housed two per cage and maintained under controlled conditions (standard 12 hour light-dark cycle, 22°C, and 21% humidity). They were allowed free access to standard rodent chow (Harlan Tekiad Lab Diet LM-485) and water. All experiments utilizing animals were conducted according to protocols approved by the Virginia Commonwealth University Institutional Animal Care and Use Committee using National Institutes of Health Guidelines for Animal Care and Use.

Preparation of intestinal microsomes. After isoflurane anesthesia, rats were guillotined. The entire intestine from the pylorus to the distal colon was rapidly removed and placed on a bed of ice. All subsequent steps in tissue handling and microsome preparation were performed at 4 °C. The duodenum was defined as the first 10 cm of intestine distal to the stomach. The remainder of the small intestine extending to the cecum was divided into four equal segments which were designated as S-1, S-2, S-3, and S-4 with S-1 being most proximal and S-4 most distal. The colon corresponded to the 10 cm segment immediately distal to the cecum. All segments were flushed with ice-cold isotonic phosphate-buffered saline containing 0.25 mM PMSF to remove intestinal contents. Mucosal epithelial cells were obtained by slitting the tissue longitudinally, scraping the epithelial, luminal side with a glass microscope slide, and collecting the scrapings in 30 mL ice-cold 0.25 M sucrose containing protease inhibitors as indicated in Table 1. In two cases (protocol C and protocol F), the scrape step was omitted and the intestinal segment samples were minced with scissors prior to homogenization. The following protease inhibitor stocks were prepared and stored at –20°C between use: PMSF (0.1 M in ethanol), EDTA (0.5 M in water), leupeptin (5 mg/mL in water), and 250X protease inhibitor cocktail (25 μg/mL pepstatin A, 25 μg/mL chymostatin, 25 μg/mL antipain, 25 μg/mL leupeptin, and 10 μg/mL aprotinin in 1% DMSO). Soybean trypsin inhibitor (50 mg/mL in phosphate-buffered saline) was prepared fresh for each experiment. Samples were homogenized in Potter-Elvehjem glass tubes using a drill-driven, serrated teflon pestle (4 passes) and then centrifuged at 18,800 x g for 15 min at 4°C. The supernatants were filtered through a loose cotton plug into a 30 mL

ultracentrifuge tube on ice and recentrifuged at 100,000 x g for 30 min at 4°C. The microsome pellets were resuspended in 0.1 M potassium phosphate buffer (pH 7.5) containing 1 mM EDTA, 20% glycerol and the indicated protease inhibitors (Table 1). Microsomes from rat liver and kidney were prepared as previously described (Kessler and Ritter, 1997). Microsomal protein concentration was estimated by the bicinchoninic acid method using a commercially available kit (Pierce Biochemical, Rockford, IL).

***In vitro* MPA Glucuronidation Assays.** MPA UGT reactions (50 µL) contained 75mM Tris-Cl (pH 7.45), 10mM $MgCl_2$, 6 mM saccharic acid 1,4-lactone, 50 µg alamethicin/mg protein, 1 mM MPA, and 1 mg/mL microsomal protein. Reactions were pre-incubated at 37°C for 3 min and were started by the addition of UDP-glucuronic acid (3mM final concentration). After 30 min at 37°C, the reactions were stopped by addition of 70% perchloric acid (5.6% final concentration). Tubes were placed on ice for 5 min and then centrifuged at 16,000 x g for 5 min. A 20 µL aliquot was then analyzed by reverse-phase high performance liquid chromatography (HPLC) as described (Wiwattanawongsa *et al.*, 2001). The HPLC system consisted of a Hewlett Packard 1050 HPLC with a Partisil 10 ODS-2 C_{18} column [4.6 mm x 25 cm] (Whatman Inc., NJ) and a Waters Resolve C_{18} Guard Pak precolumn cartridge (Millipore, MA). The mobile phase was 55% MeOH/45% aqueous trifluoroacetic acid (0.1% TFA). The flow rate was 1.5 ml/min. Absorbance was monitored with a Hewlett Packard 1050 diode array detector set at 250 nm. Under our conditions, the retention times for MPAG, the suprofen internal standard, and MPA were 3.3, 8.8, and 11.8 min, respectively. MPAG was quantitated using standard curves prepared using blank microsome reactions spiked with known amounts

of authentic MPAG standard. Care was taken to perform all reactions under conditions when MPAG formation was linearly proportional to time and protein concentration. The limit of detectable activity of our assay was ~ 0.010 nmol/mg/min.

Kinetic Analysis of MPA K_m and V_{max}. Michaelis-Menten enzyme kinetic parameters were determined by assessing the effect of MPA concentration (varied between 0.01 and 1 mM) on the rate of MPAG formation. Concentrations >1 mM were found to inhibit the MPAG reaction. The kinetic constants K_m and V_{max} were estimated by non-linear regression using WinNonlin™ pharmacokinetic software v. 2.0 (Pharsight Corporation, Palo Alto, CA).

Preparations of recombinant expressed rat UGTs. HepG2 cells were grown to 90-95% confluence in Dulbecco's modified Eagle's medium supplemented with 10% fetal calf serum, at which time individual plates were infected with adenovirus lysates encoding the UGTs indicated. Cells were harvested by gentle pipetting to release cells 72 hr after infection and centrifuging at 5000 rpm in a clinical centrifuge at 4°C. Supernatants were discarded, and the resulting cell pellets were washed by resuspension in ice-cold 1X phosphate-buffered saline and recentrifugation. The washed cell pellets were resuspended in 0.1 M potassium phosphate buffer, pH 7.5, 20% glycerol, and 1 mM EDTA. After three consecutive freeze/thaw cycles and a brief sonication to disperse aggregates, the cells were centrifuged at 5000 x g for 10 min. The supernatants were collected and transferred to microfuge tubes. Protein concentration was determined as described above. Membrane preparations were aliquotted and stored at -80°C until assay.

Immunoblot analysis of UGT1A1, 1A6, 1A7-like, and total UGT1A protein. Relative and absolute amounts of UGT1A proteins were determined using an immunoblotting procedure previously described (Ritter *et al.*, 1999; Kessler *et al.*, 2002) with some modifications. Microsomal protein (30 μg) was electrophoresed in parallel with serial dilutions of the desired recombinant expressed rat UGTs on a 7.5% SDS-polyacrylamide gel and transferred onto a nitrocellulose membrane. The blots were probed using antisera raised in mice against bacterial-expressed UGT fusion proteins. The latter represent amino acid residues 29-162 (UGT1A1), 77-183 (UGT1A6), 21-149 (UGT1A7), and 360-455 (rat UGT1A common region), respectively. The specificities of these antisera have been established (Kessler *et al.*, 2002; Webb *et al.*, 2005a; Webb *et al.*, 2005b). While the 1A1 and 1A6 antisera exhibit high specificity for their respective enzymes, the 1A7 antiserum cross-reacts weakly with 1A8 (Kessler *et al.*, 2002), and the immunoreactivity with this antiserum is therefore designated as being UGT1A7-like. The rat UGT1A common region antibody shows complete specificity for UGT1A versus UGT2 enzymes (Webb *et al.*, 2005b). For quantitative immunoblotting, a previously described procedure was used (Kessler *et al.*, 2002). Proteins were detected using enhanced chemiluminescence (ECL) (Amersham Biosciences, Piscataway, NJ). Images were captured on film and quantified using Image J™ (freeware available at http://rsb.info.nih.gov/ij/). All calculations were based on recombinant rat UGT standards, which were used to generate standard curves.

Data analysis. Data were analyzed by ANOVA testing using Sigma Stat™ v. 2.03 software (SPSS Inc., Chicago, IL). When differences between groups were found, a Student-Newman Keuls posthoc test was used to identify specific groups showing differences. A p value <0.05 was considered to be statistically significant. Correlation analyses were performed using Spearman's rank order correlation test.

Results

Evaluation of protease inhibitors used in the preparation of intestinal microsomes.

Comparison of intestinal microsome glucuronidation data between different laboratories is complicated by the lability of intestinal UGT activities, a problem stemming from the contamination of intestinal preparations with proteases. While the inclusion of protease inhibitors has been standard in protocols for preparing intestinal microsomes, both the types and amounts of protease inhibitors used have varied among laboratories. A systematic study was therefore performed to compare the efficacies of different protease inhibitors and protease inhibitor combinations, including two of the standard protease inhibitors described in the literature, PMSF and soybean trypsin inhibitor (Table 1). Protocols B and C, which included soybean trypsin inhibitor at 5 mg/g wet weight, yielded higher MPAG formation rates (2.4 to 3.1 nmol/min/mg) compared to protocols lacking soybean trypsin inhibitor (Fig. 1A). Reduced proteolytic digestion of UGT (detected either by the loss of intact UGT protein or the appearance of immunoreactive degradation products) was also evident in immunoblot analyses of the samples prepared using soybean trypsin inhibitor (Lanes B and C of Fig. 1B). These data suggested that the methods using the combination of soybean trypsin inhibitor with PMSF (protocols B and C) were superior to those relying on PMSF (protocols D and E).

However, even in the samples prepared using the combination of soybean trypsin inhibitor and PMSF, a problem with stability of the MPA UGT activity was evident. Loss of MPA UGT activity was observed upon freezing and thawing of the samples or by storing the microsomes on ice overnight. Representative results are shown in Fig. 2 (top panel) for duodenum and S-1 microsomes prepared using protocol C. The duodenal

microsomes exhibited a 10% decrease in the activity after overnight incubation on ice, whereas >20% was lost by a single freeze-thaw cycle. S-1 microsomes showed a more dramatic effect with an 80% reduction in MPA UGT activity after either overnight incubation on ice or a single freeze-thaw cycle. The observed instability of MPA UGT activity of S-1 microsomes was also evident over the time course of a 30 min reaction at 37°C (Fig. 2, bottom panel). The susceptibility to inactivation by freezing and thawing and incubations on ice for extended periods varied between segments. It appeared greatest for microsomes prepared from upper small intestine segments, especially S-1 and S-2. Duodenum and S-3 showed an intermediate degree of instability, whereas S-4 and colon appeared refractory (data not shown). These data overall suggested that microsomes prepared from the small intestine of rats have residual protease contamination, and that the more proximal segments have the greatest contamination.

To address the lability issue, a combination protease method was tested, which included PMSF, soybean trypsin inhibitor and a more concentrated protease inhibitor cocktail containing aprotinin, pepstatin A, chymostatin, leupeptin, and antipain (see protocol F in Table 1). Representative results are presented in Fig. 2 (middle panel). Microsomal MPA UGT activities from duodenum, S-1, S-2 and S-3 were completely stabilized using this combination of protease inhibitors (data shown only for duodenum and S-1). No effect of either freezing/thawing (up to 5 cycles) or time of incubation on ice was evident in any of the samples. Moreover, the time course of MPAG formation catalyzed by S-1 microsomes prepared by this protocol was linear.

Distribution of MPA UGT activity along the small intestine and colon. Using the optimized intestinal microsome preparation method (protocol F), we examined the distribution of MPA UGT activity along the male Sprague-Dawley rat small intestine (Fig. 3). Chromatograms of intestinal microsome incubations showed only a single apparent MPA glucuronidation product, which co-eluted with authentic MPA-7-O-glucuronide (data not shown). MPAG formation rates showed a longitudinal gradient along the gastrointestinal tract, with the highest activities observed toward the upper end of the small intestine (including duodenum, S-1 and S-2) and progressively lower activities in the lower segments of small intestine and the colon. In comparison, kidney microsomes had intermediate MPA UGT activity, and liver microsomes had high activity, comparable to S-1 intestinal microsomes (8-12 nmol/mg/min rates).

The kinetic properties of MPA UGT activity along small intestine were characterized in experiments that determined the influence of MPA concentration (0.0156-1 mM) on the MPAG formation rate. All microsomes exhibited concentration-dependent glucuronidation that fit the standard Michaelis-Menten model as assessed using Winnonlin™ enzyme kinetics modeling software. Average V_{max} and K_m values determined for small intestine segments and colon of three male rats are presented in Table 2. For comparison, the V_{max} and K_m for rat liver microsomal MPA UGT were 6.7 +/- 1.1 nmol/mg/min and 0.20 +/- 0.02 mM, respectively (Miles *et al.*, 2005). Each parameter varied along the intestine, with V_{max} decreasing from duodenum to colon in a manner paralleling the MPA UGT activities determined at 1 mM MPA (Fig. 3), and K_m increasing significantly down the length of the small intestine. Due to the reciprocal nature of the changes, the V_{max}:K_m ratio (an index of intrinsic clearance) decreased

markedly along the small intestine, from a high of 180 in the duodenum to a low of 16 in the S-3 segment. Colon also exhibited a low V_{max} to K_m ratio.

The MPA UGT activities of heterozygous and homozygous male Gunn rats (genotypes j/+ and j/j, respectively) were also evaluated to assess the role of UGT1A enzymes in the intestinal activity. No activity was detected with any of the intestine or colon samples prepared from homozygous Gunn rats (<0.03 nmol/mg/min). HPLC chromatograms illustrating this effect using duodenum microsomes are shown in Fig. 4. The corresponding rate data are presented in Fig. 5 (left panel). Samples from heterozygote (j/+) rats exhibited activities intermediate between Sprague-Dawley and homozygous Gunn rats. A Spearman rank order correlation test revealed a highly significant correlation between genotype and intestinal MPA UGT activity (Fig. 5, right panel). These data indicate that the MPA UGT activity in rat small intestine is constituted completely by UGT1A family enzymes with no UGT2B contribution. Since our previous study revealed MPAG-forming activity of only three rat UGT1A family enzymes, i.e., the UGT1A1, 1A6, and 1A7 forms (Miles *et al.*, 2005), the results suggest that one or more of these three enzymes are responsible for the intestinal MPAG activity.

To further evaluate this question, quantitative immunoblotting was conducted to assess differences in the absolute content of UGT1A1, 1A6, and 1A7-like enzymes in rat intestine as well as kidney and liver microsomes. For quantitative western blotting, our approach extended a method described previously by our laboratory for estimating the 1A7-like content of rat liver microsomes (Kessler *et al.*, 2002). Application of the method allowed for the determination of 1A7 in a preparation of UGT1A7 in recombinant adenovirus-infected HepG2 cells (34 μg/mg, data not shown). This

standardized preparation of HepG2-r1A7 was subsequently used to estimate the contents of 1A1 and 1A6 in two other preparations of HepG2 expressing rat 1A1 and 1A6. Each was normalized to the HepG2-r1A7 preparation using a rat UGT1A common region antiserum (r1CR) generated in this laboratory, which is assumed to recognize all UGT1A enzymes with equal efficiency. The approach of using a UGT1A common region to assess relative levels of UGT1A enzyme expression has been widely used by investigators in the glucuronidation field (Gagne *et al.*, 2002; Basu *et al.*, 2004). The content of 1A1 and 1A6 in microsomes prepared from HepG2 cells infected for 72 h with adenoviruses expressing rat 1A1 and 1A6, respectively was determined to be 36 and 21 μg/mg, respectively (data not shown).

Using the recombinant rat UGT-expressing HepG2 cell microsomes as standards in conjunction with the antisera to rat UGT1A1, 1A6 and 1A7, quantitative immunoblotting was applied toward analysis of microsomes prepared from different tissues of male Sprague-Dawley rats (n=3). The cumulative quantitative data are presented in Fig. 6. Representative immunoblots for the intestine samples (excluding the recombinant UGT standards) are shown for each antiserum. The major UGT expressed in intestine was a UGT1A7-like enzyme. Its content declined sharply along the intestine, from a peak of 23.8 μg/mg in S-1 microsomes to a low value of 7.3 μg/mg in colon ($p<0.05$). The 1A7-like content in kidney and liver microsomes was several fold lower than colon. The 1A1 content was more even along the duodenum, S-1, S-2, and S-3 with a slight elevation apparent in S-4 and colon (not statistically significant). In contrast to the 1A7-like expression profile, the kidney and liver content of 1A1 were much higher than that of intestine. A third distinct pattern of expression was observed for the 1A6

enzyme. The 1A6 content was roughly equal across all tissues. Although slightly higher levels were evident in the colon, liver, and kidney, the 1A6 content was not found to differ statistically.

Given the apparent correspondence between UGT1A7-like protein content and MPA UGT activity, the data were also analyzed by the Spearman rank order correlation test (Fig. 7). The MPA UGT activity of rat intestine was highly correlated with UGT1A7-like content ($p = 0.001$), whereas no correlation was evident with the content of either UGT1A1 ($p = 0.86$) or UGT1A6 ($p = 0.84$).

Discussion

This study characterized the MPA UGT activity of rat intestine, which may act to modulate the gastrointestinal toxicity associated the use of MMF. Several findings of interest were uncovered, including the demonstration of high catalytic activity of rat intestinal microsomes towards MPA, the presence of a distinct distribution pattern in the activity as well as in kinetic properties for MPA glucuronidation (V_{max}, K_m, and V_{max}/K_m ratio), the strong parallel observed between MPAG formation rates and the content of a UGT1A enzyme detected with a UGT1A7-selective antibody (presumably UGT1A7 itself), and the finding at the protein level that not all UGT isoforms are distributed in the same pattern along the gastrointestinal tract.

The demonstration of high catalytic activity towards MPA, a phenolic substrate, is consistent with data from early studies indicating that rat intestinal microsomes are quite active (>1 nmol/mg/min) in the glucuronidation of substrates with phenolic -OH groups, such as *o*-aminophenol, 4-nitrophenol, 1-naphthol and 2-naphthol, 4-methylumbelliferone, and morphine (Hietanen *et al.*, 1972; Hietanen and Vainio, 1973; Koster *et al.*, 1985; Vargas and Franklin, 1997). Moreover, several of these studies examined the distribution of the phenol glucuronidating activities along the gastrointestinal tract. Although direct comparisons are difficult due to differences in the intestinal microsome preparation methods and the way in which the intestine was divided into segments, a common feature of these reports is the observation of a gradual decline in UGT activity from the duodenum to the large bowel. This decline in activity was also apparent in our study for MPA.

The characterization of kinetic parameters for MPA glucuronidation along the intestine was a unique aspect of this study. The kinetic analysis indicates that the decline in MPA UGT activity observed under standard MPA UGT reaction conditions (including 1 mM MPA and 3 mM UDP-glucuronic acid, see Fig. 3) was attributable to changes in both V_{max} and K_m. The progressive decrease in V_{max} observed between the duodenum, S-2, and colon (Table 2) suggests that the content of an MPA UGT or UGTs is reduced as one proceeds along the intestine The association of the effect with an increase in K_m (decreased affinity) of the MPA UGT(s) for MPA may be explained by multiple UGTs contributing to MPA catalysis. These UGTs would have different V_{max} and K_m for MPA glucuronidation, and the different ratios of V_{max} to K_m would be a consequence of differential changes in their expression along the length of the intestine.

Because Gunn (j/j) rat intestinal microsomes exhibited no detectable MPA UGT activity, the data demonstrate that UGT1A family enzymes catalyze all MPA UGT activity and that UGT2B enzymes have an insignificant role in naive rat intestine. This result contrasts with the MPA UGT activity of rat liver, which has a small but significant UGT2B component (estimated to be between 10-20% of the total activity measured under standard reaction conditions). During screens of recombinant rat UGT1A and 2B enzymes for catalytic activity towards MPA (Miles *et al*., 2005), three active enzymes were identified: UGT1A7, a high affinity-high capacity MPA-metabolizing enzyme (V_{max} 10.3 nmol/mg/min and K_m= 0.034 mM); UGT1A1, an intermediate affinity and capacity enzyme (V_{max} = 1.7 nmol/mg/min and K_m 0.21 mM); and UGT1A6, a low affinity/intermediate capacity enzyme (V_{max} = 1.3 nmol/mg/min and K_m = 1 mM). Results from UGT1A mRNA analyses show detectable expression of each of these

enzymes in rat intestine, raising the question about their relative quantitative roles in the intestinal catalysis of MPA glucuronidation.

It appears likely that UGT1A7 is the major enzyme mediating rat intestinal MPA glucuronidation, particularly in the upper small intestine if not also the more distal segments and the colon. One line of evidence is the correlation observed between MPAG formation rate and the UGT immunoreactivity detected with a UGT1A7-selective polyclonal antiserum. Although we cannot directly exclude the possibility, it does not appear that rat UGT1A8 or UGT1A10 are significant contributors to the 1A7-like immunoreactivity of intestine, based on several recent studies showing high abundance of the UGT1A7 transcript in rat intestine (Kobayashi *et al.*, 1998; Grams *et al.*, 2000; Shelby *et al.*, 2003; Webb *et al.*, 2005a). In contrast, Shelby *et al*. reported detectable expression of the UGT1A8 mRNA in liver, kidney, and colon but not small intestine (Shelby *et al.*, 2003). The same pattern of low UGT1A8 mRNA expression in liver and kidney and undetectable expression in intestine was confirmed in a recent study by our laboratory using an alternative approach (RNAse protection analysis) (Webb *et al.*, 2005a). A parallel analysis of UGT1A10 mRNA in the same study (data not shown) revealed a profile similar to 1A8, with low levels in liver and kidney and undetectable levels in intestine.

The current report is the first to our knowledge to provide quantitative estimates of the UGT content of rat liver, kidney, and intestinal microsomes as well as to describe the longitudinal distribution of specific UGT enzymes along the rat gastrointestinal tract. Of the three enzymes studied, UGT1A7 was quantitatively the most abundant UGT in the intestine with much lower levels in the liver and kidney, and it was the only one of the

three enzymes active towards MPA to show a marked longitudinal gradient in expression. Two different studies have evaluated the distribution of UGT1A7 mRNA along the rat gastrointestinal tract and its tissue specificity (Grams *et al.*, 2000; Shelby *et al.*, 2003). Both studies observed declines in UGT1A7 expression along the length of the intestine, which is consistent with our protein level data. In addition, both studies noted more abundant expression of UGT1A7 in the intestine versus the kidney and liver. Taken together, the data suggest that the mechanism underlying the proximal to distal gradient in UGT1A7 activity is transcriptional in origin.

This study establishes for the first time the presence of 1A1 and 1A6 protein in the rat gastrointestinal tract. However, their levels were much lower than that of 1A7-like enzyme, and each showed lower variation along the intestine. A strong contrast was also evident in their expression across liver, kidney, and intestine. UGT1A1 exhibited a much higher level in liver compared to kidney and intestine, whereas UGT1A6 was more evenly expressed across all three tissues. Our data suggesting the absence of a significant gradient of 1A1 and 1A6 protein along the gastrointestinal tract is in general agreement with the results of mRNA analysis (Grams *et al.*, 2000; Shelby *et al.*, 2003), with neither study noting any evidence for any longitudinal variation in their expression. However, our finding of much higher UGT1A1 abundance in liver versus intestine contrasts with the mRNA analysis data (Shelby *et al.*, 2003), which indicated fairly even expression of UGT1A1 mRNA across these tissues (2-fold range in variation). The reason for this difference remains unclear but may be explained by tissue-specific differences in the efficiencies of UGT1A1 mRNA translation or protein degradation.

Overall, our results suggest the following model for MPA glucuronidation catalyzed by rat intestine. MPA glucuronidation is highest in the duodenum and other proximal segments of rat intestine, an effect related to the high expression in these tissues of UGT1A7, a high affinity/high MPA-metabolizing enzyme. UGT1A1 and UGT1A6 are also predicted to contribute to the total activity in the upper intestine but quantitatively their influence is minor. In the more distal small intestine, as UGT1A7 enzyme levels decline, the efficiency of MPA catalysis decreases. The observed increase in K_m of the lower rat small intestine and colon for MPA UGT may be due to an increased relative contribution of UGT1A1 and UGT1A6, low affinity MPA-metabolizing UGTs. This interpretation is supported by the upward shift in the K_m of rat liver microsomes for MPA (0.2 mM). In liver, the UGT1A1 and 1A6 forms are more abundant than 1A7 (Fig. 6).

It is of interest to consider the relationship of our rat intestinal UGT expression data to human. Although intestinal microsomes from both species catalyze MPA glucuronidation at high rates (Bowalgaha and Miners, 2001; Shipkova *et al.*, 2001; Bernard and Guillemette, 2004; Picard *et al.*, 2005), differences are likely to exist in the UGTs responsible for MPA catalysis in rat versus human intestine. With human intestine, MPA UGT activity is unlikely to be dominated by UGT1A7, which exhibits low expression in human intestine and colon (Tukey and Strassburg, 2001). However, it does appear though that the intestinal MPA UGT activity in the two species shares the characteristic of being dominated by UGT1A enzymes in the "bulky phenol" UGT1A7-1A10 subfamily. Human UGT1A8 and 1A10 are expressed in human intestine and are active in MPA catalysis (Mojarrabi and Mackenzie, 1997; Mackenzie, 2000).

In summary, the current study enhances our understanding of intestinal MPA glucuronidation in rats. This knowledge will be useful for future studies using the rat model to assess the influence of intestinal UGT expression on MPA-induced gastrointestinal toxicity.

References

Basu, N. K., S. Kubota, M. R. Meselhy, M. Ciotti, B. Chowdhury, M. Hartori and I. S. Owens (2004). Gastrointestinally distributed UDP-glucuronosyltransferase 1A10, which metabolizes estrogens and nonsteroidal anti-inflammatory drugs, depends upon phosphorylation. J Biol Chem **279**: 28320-9.

Bernard, O. and C. Guillemette (2004). The main role of UGT1A9 in the hepatic metabolism of mycophenolic acid and the effects of naturally occurring variants. Drug Metab Dispos **32**: 775-8.

Bowalgaha, K. and J. O. Miners (2001). The glucuronidation of mycophenolic acid by human liver, kidney and jejunum microsomes. Br J Clin Pharmacol **52**: 605-9.

Bullingham, R. E., A. J. Nicholls and B. R. Kamm (1998). Clinical pharmacokinetics of mycophenolate mofetil. Clin Pharmacokinet **34**: 429-55.

Busca, A., F. Locatelli and M. Falda (2001). Safety profile of mycophenolate mofetil: a response. Bone Marrow Transplant **27**: 892.

Dutton, G. J. (1980). Glucuronidation of drugs and other compounds. Boca Raton, FL, CRC Press.

Fisher, M. B., M. F. Paine, T. J. Strelevitz and S. A. Wrighton (2001). The role of hepatic and extrahepatic UDP-glucuronosyltransferases in human drug metabolism. Drug Metab Rev **33**: 273-97.

Gagne, J. F., V. Montminy, P. Belanger, K. Journault, G. Gaucher and C. Guillemette (2002). Common human UGT1A polymorphisms and the altered metabolism of irinotecan active metabolite 7-ethyl-10-hydroxycamptothecin (SN-38). Mol Pharmacol **62**: 608-17.

Grams, B., A. Harms, S. Braun, C. P. Strassburg, M. P. Manns and P. Obermayer-Straub (2000). Distribution and inducibility by 3-methylcholanthrene of family 1 UDP-glucuronosyltransferases in the rat gastrointestinal tract. Arch Biochem Biophys **377**: 255-65.

Gregory, P. A., R. H. Lewinsky, D. A. Gardner-Stephen and P. I. Mackenzie (2004). Regulation of UDP glucuronosyltransferases in the gastrointestinal tract. Toxicol Appl Pharmacol **199**: 354-63.

Hietanen, E., A. Aitio and O. Hanninen (1972). Studies on the control of glucuronide synthesis in the rat small intestine. Acta Pharmacol Toxicol (Copenh) **31**: 186-92.

Hietanen, E. and H. Vainio (1973). Interspecies variations in small intestinal and hepatic drug hydroxylation and glucuronidation. Acta Pharmacol Toxicol (Copenh) **33**: 57-64.

Kessler, F. K., M. R. Kessler, D. J. Auyeung and J. K. Ritter (2002). Glucuronidation of acetaminophen catalyzed by multiple rat phenol UDP-glucuronosyltransferases. Drug Metab Dispos **30**: 324-30.

Kessler, F. K. and J. K. Ritter (1997). Induction of a rat liver benzo[a]pyrene-trans-7,8-dihydrodiol glucuronidating activity by oltipraz and beta-naphthoflavone. Carcinogenesis **18**: 107-14.

Kobayashi, T., H. Yokota, S. Ohgiya, H. Iwano and A. Yuasa (1998). UDP-glucuronosyltransferase UGT1A7 induced in rat small intestinal mucosa by oral administration of 2-naphthoflavone. Eur J Biochem **258**: 948-55.

Koster, A. S., A. C. Frankhuijzen-Sierevogel and J. Noordhoek (1985). Distribution of glucuronidation capacity (1-naphthol and morphine) along the rat intestine. Biochem Pharmacol **34**: 3527-32.

Mackenzie, P. I. (2000). Identification of uridine diphosphate glucuronosyltransferases involved in the metabolism and clearance of mycophenolic acid. Ther Drug Monit **22**: 10-3.

Miles, K. K., S. T. Stern, P. C. Smith, F. K. Kessler, S. Ali and J. K. Ritter (2005). An investigation of human and rat liver microsomal mycophenolic Acid glucuronidation: evidence for a principal role of ugt1a enzymes and species differences in ugt1a specificity. Drug Metab Dispos **33**: 1513-20.

Mojarrabi, B. and P. I. Mackenzie (1997). The human UDP glucuronosyltransferase, UGT1A10, glucuronidates mycophenolic acid. Biochem Biophys Res Commun **238**: 775-8.

Picard, N., D. Ratanasavanh, A. Premaud, Y. Le Meur and P. Marquet (2005). Identification of the udp-glucuronosyltransferase isoforms involved in mycophenolic Acid phase ii metabolism. Drug Metab Dispos **33**: 139-46.

Ritter, J. K. (2000). Roles of glucuronidation and UDP-glucuronosyltransferases in xenobiotic bioactivation reactions. Chem Biol Interact **129**: 171-93.

Ritter, J. K., F. K. Kessler, M. T. Thompson, A. D. Grove, D. J. Auyeung and R. A. Fisher (1999). Expression and inducibility of the human bilirubin UDP-glucuronosyltransferase UGT1A1 in liver and cultured primary hepatocytes: evidence for both genetic and environmental influences. Hepatology **30**: 476-84.

Shelby, M. K., N. J. Cherrington, N. R. Vansell and C. D. Klaassen (2003). Tissue mRNA expression of the rat UDP-glucuronosyltransferase gene family. Drug Metab Dispos **31**: 326-33.

Shipkova, M., C. P. Strassburg, F. Braun, F. Streit, H. J. Grone, V. W. Armstrong, R. H. Tukey, M. Oellerich and E. Wieland (2001). Glucuronide and glucoside conjugation of mycophenolic acid by human liver, kidney and intestinal microsomes. Br J Pharmacol **132**: 1027-34.

Tukey, R. H. and C. P. Strassburg (2001). Genetic multiplicity of the human UDP-glucuronosyltransferases and regulation in the gastrointestinal tract. Mol Pharmacol **59**: 405-14.

Vargas, M. and M. R. Franklin (1997). Intestinal UDP-glucuronosyltransferase activities in rat and rabbit. Xenobiotica **27**: 413-21.

Webb, L. J., K. K. Miles, D. J. Auyeung, F. K. Kessler and J. K. Ritter (2005a). Analysis of substrate specificities and tissue expression of rat UDP-glucuronosyltransferases UGT1A7 and UGT1A8. Drug Metab Dispos **33**: 77-82.

Webb, L. J., K. K. Miles, F. K. Kessler and J. K. Ritter (2005b). Activity of rat UGT1A1 towards benzo[a]pyrene phenols and dihydrodiols. Environmental Toxicology and Pharmacology **In Press**.

Wiwattanawongsa, K., E. L. Heinzen, D. C. Kemp, R. E. Dupuis and P. C. Smith (2001). Determination of mycophenolic acid and its phenol glucuronide metabolite in human plasma and urine by high-performance liquid chromatography. J Chromatogr B Biomed Sci Appl **763**: 35-45.

Footnotes

The following is an unnumbered footnote to the title:

This work was supported in part by NIH grants 1R01-GM61188 and 5R01-ES07762 from the National Institutes of General Medical Sciences and Environmental Health Sciences, respectively.

Reprint requests to:

Dr. Joseph K. Ritter, Department of Pharmacology and Toxicology, Box 980613, Virginia Commonwealth University School of Medicine, Richmond, VA 23298-0613.

Phone: (804) 828-1022. FAX: (804) 828-0676. Email: jkritter@vcu.edu

Figure legends

Fig. 1. Comparison of MPA UGT activities and UGT immunoblot profiles of rat intestinal microsomes prepared using different protease inhibitor combinations. Intestinal microsomes were prepared from a 25-cm segment of duodenum/proximal small intestine as described under Materials and Methods using the protocols listed in Table 1**.** A, no protease inhibitor control. B, PMSF + soybean trypsin inhibitor. C, PMSF + soybean trypsin inhibitor. D, PMSF + EDTA. E, PMSF + EDTA + 1X protease inhibitor cocktail. Mucosal scrapings were used in each case except method C which minced the tissue using scissors). Top panel, MPAG formation rates estimated in standard MPA UGT reactions containing 1 mM MPA and 3 mM UDP-glucuronic acid. The data represent the mean rate (nmol/mg/min) +/- SEM for three independent microsome preparations. The data for groups B and C are significantly different from the other groups ($p<0.05$). Bottom panel, results of SDS-PAGE western blots analyses using the indicated antisera. Note the evidence for proteolytic loss or degradation, particularly in samples prepared using protocols A, D, and E.

Fig. 2. Stabilization of intestinal microsomal UGT activity using a multiple protease inhibitor approach. Top panel, MPA UGT activities of microsomes prepared from duodenum or S-1 using protocol C. Middle panel, MPA UGT activities of microsomes prepared using protocol F. In each case, the microsomes were assayed for MPA UGT activity immediately after preparation ("Fresh"), after one or five freeze-thaw cycles ("1X or 5X Thaw") or after an overnight incubation on ice ("O/N ice"). Bottom panel, time course of MPAG formation of S-1 microsomes prepared by protocol C (△—△) or

protocol F (○—○). All reactions were conducted under standard conditions: 1 mg/mLmicrosomal protein, 50 μg alamethicin/mg protein, 1 mM MPA, and 3 mM UDP-glucuronic acid at 37°C.

Fig. 3. Microsomal MPA UGT activities of male Sprague Dawley rat small intestine, colon, kidney, and liver. MPA UGT activities were measured using 1 mg/mL microsomal protein, 50 μg alamethicin/mg protein, 6 mM δ-saccharic acid 1,4-lactone, 1 mM MPA, and 3 mM UDP-glucuronic acid at 37°C for 30 min. The results represent the mean MPAG formation rate (expressed as nmol/mg/min) +/- SEM of either four (colon, kidney, liver) or six (duodenum, S-1, S-2, S-3, and S-4) male Sprague-Dawley rat microsome preparations. [a] $p<0.05$ versus duodenum sample. [b] $p<0.05$ versus S-3 sample. [c] $p<0.05$ versus colon sample. [d] $p<0.05$ versus liver sample. [e] $p<0.05$ versus kidney sample.

Fig. 4. Effect of the Gunn rat genotype on the HPLC chromatographic profiles of intestinal MPA UGT reactions. Duodenal microsomes from male rats of the strain indicated were assayed for MPA UGT activity as described under **Materials and Methods**. Aliquots of the reaction supernatants were subjected to HPLC analysis with detection at 250 nm. Peak 1 is MPAG, peak 2 is the internal standard (suprofen), and peak 3 is uncojugated MPA. Note the complete absence of peak 1 in reactions containing homozygous Gunn (j/j) microsomes.

Fig. 5. Effect of genotype at the UGT1A locus on intestinal MPAG formation rates. Microsomes were prepared from the indicated small intestinal segments or colon of male heterozygous Gunn (j/+), homozygous (j/j) Gunn, or Sprague Dawley rats and assayed for MPA UGT activity as described under **Materials and Methods**. Left panel, MPAG formation rates are expressed as nmol MPAG formed/min/mg. UGT activities were determined at 1 mM MPA and 3 mM UDP-glucuronic acid. Two rats of each genotype/strain were analyzed. Right panel, plot showing the dependence of MPA UGT activity on the genotype at the UGT1A locus. The r^2 and p values are from Spearman rank order correlation analysis.

Fig. 6. Quantitative immunoblot analysis of three MPA-metabolizing rat UGT1A family members. Microsomal protein from the different segments of small intestine, the colon, the kidney, and the liver was analyzed for the contents of UGT1A1 (left panel), UGT1A6 (middle panel), or UGT1A7-like protein (right panel) using a quantitative immunoblotting approach. Bar graphs represent the average enzyme contents ± SEM in units of ng UGT protein/μg microsomal protein of three male Sprague Dawley rats. A representative immunoblot from an individual rat (excluding the recombinant standard samples) is shown at the top of each panel. ^{a} $p<0.05$ versus duodenum sample. ^{b} $p<0.05$ versus S-3 sample. ^{c} $p<0.05$ versus colon sample. ^{d} $p<0.05$ versus liver sample.

Fig. 7. Correlation of MPA UGT activity versus UGT1A1, 1A6, and 1A7-like content of rat intestinal microsomes. MPA UGT activities of duodenum, S-1, S-2, S-3, S-4, and colon microsomes from three male Sprague-Dawley rats were determined and

plotted against their estimated contents of UGT1A1 (left panel), UGT1A6 (middle panel), or UGT1A7-like protein (right panel) determined for each sample by quantitative immunoblotting. The best-fit line estimated by least squares linear regression is shown. The coefficient of regression r^2 and p value shown were obtained by Spearman rank order correlation analysis.

Tables

Table 1

Tissue processing and protease inhibitor combinations used in intestinal microsome preparations

Protocol	Tissue processing	Protease inhibitor additions	
		Tissue homogenization buffer	**Microsome resuspension buffer**
A	Scraping	None	1 mM EDTA
B	Scraping	0.1 mM PMSF 5 mg trypsin inhibitor/g wt weight	1 mM EDTA 0.1 mM PMSF
C	Mincing	0.1 mM PMSF 5 mg trypsin inhibitor/g wt weight	1 mM EDTA 0.1 mM PMSF
D	Scraping	1 mM EDTA 0.25 mM PMSF 0.1 mM dithiothreitol	1 mM EDTA 0.1 mM PMSF 5 μg/mL Leupeptin
E	Scraping	1 mM EDTA 0.1 mM PMSF 1X Protease Inhibitor Cocktail[a]	1 mM EDTA 0.1 mM PMSF 1X Protease Inhibitor Cocktail[a]

F	Mincing	1 mM EDTA	1 mM EDTA
		0.1 mM PMSF	0.1 mM PMSF
		5 mg trypsin inhibitor/g wt weight	0.1 mg/mL trypsin inhibitor
		5X Protease Inhibitor Cocktail[b]	5X Protease Inhibitor Cocktail[b]

[a]Contains the protease inhibitors (pepstatin A, chymostatin, antipain, leupeptin) at 0.1 μg/mL, and aprotinin at 0.04 μg/mL.

[b]Contains the protease inhibitors (pepstatin A, chymostatin, antipain, leupeptin) at 0.5 μg/mL, and aprotinin at 0.2 μg/mL.

DMD Fast Forward. Published on June 21, 2006 as DOI: 10.1124/dmd.106.010140
This article has not been copyedited and formatted. The final version may differ from this version.

Table 2

Michaelis Menten kinetic parameters determined for MPAG formation catalyzed by rat intestine microsomes[a]

MPA UGT activities of microsomes prepared from the indicated intestinal segments of adult male Sprague-Dawley rats were analyzed as described under **Materials and Methods,** and kinetic parameters were determined. The V_{max} to K_m is included as a measure of intrinsic clearance. Results represent the average ± SEM of three independent preparations

Intestinal Segment	n	K_m (mM)	V_{max} (nmol/mg/min)	V_{max}/K_m (μL/mg/min)
Duodenum	3	0.067 ± 0.026	7.68 ± 0.29	180 ± 28
S-1	3	0.056 ± 0.013	7.81 ± 1.56	143 ± 26
S-2	3	0.091 ± 0.015	6.01 ± 0.37[a]	70 ± 13[a]

S-3	3	0.160 ± 0.022[a]	2.48 ± 0.43	16 ± 5
S-4	3	0.103 ± 0.022	3.16 ± 0.40[b]	33 ± 8[b]
Colon	3	0.158 ± 0.004 [a,b]	3.20 ± 0.17[b]	20 ± 1[b]

[a] $p < 0.05$ compared to duodenum group.

[b] $p < 0.05$ compared to S-2 group.

DMD Fast Forward. Published on June 21, 2006 as DOI: 10.1124/dmd.106.010140
This article has not been copyedited and formatted. The final version may differ from this version.

Figure 1

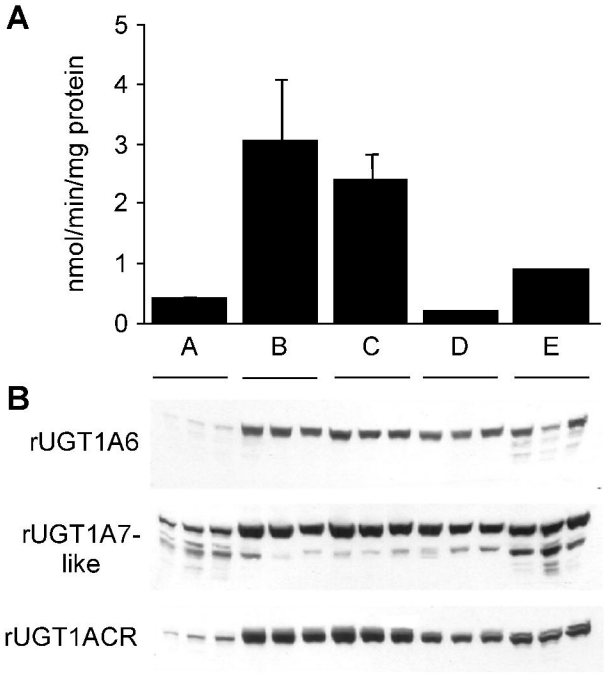

DMD Fast Forward. Published on June 21, 2006 as DOI: 10.1124/dmd.106.010140
This article has not been copyedited and formatted. The final version may differ from this version.

Figure 2

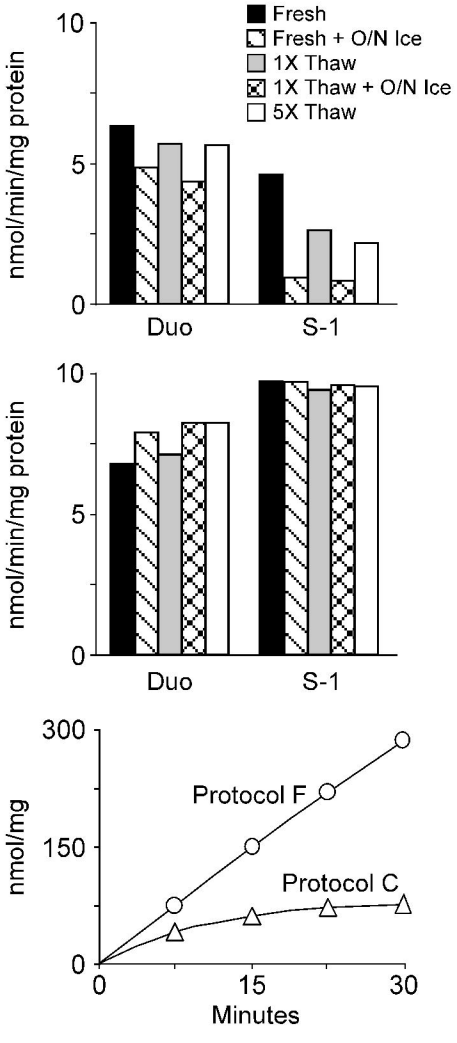

DMD Fast Forward. Published on June 21, 2006 as DOI: 10.1124/dmd.106.010140
This article has not been copyedited and formatted. The final version may differ from this version.

Figure 3

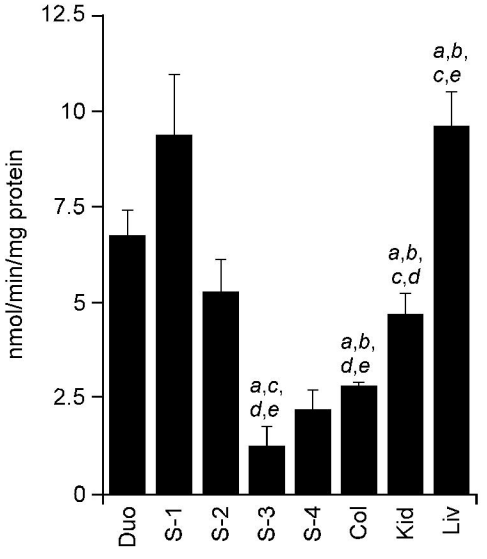

DMD Fast Forward. Published on June 21, 2006 as DOI: 10.1124/dmd.106.010140
This article has not been copyedited and formatted. The final version may differ from this version.

Figure 4

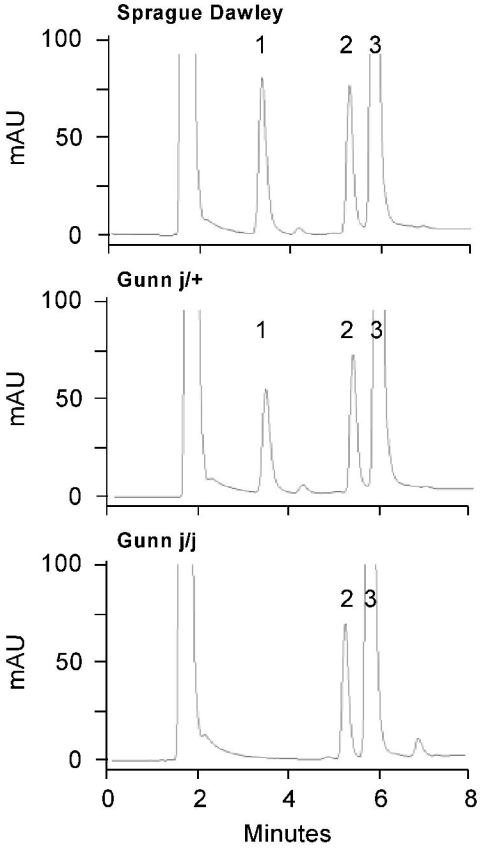

DMD Fast Forward. Published on June 21, 2006 as DOI: 10.1124/dmd.106.010140
This article has not been copyedited and formatted. The final version may differ from this version.

Figure 5

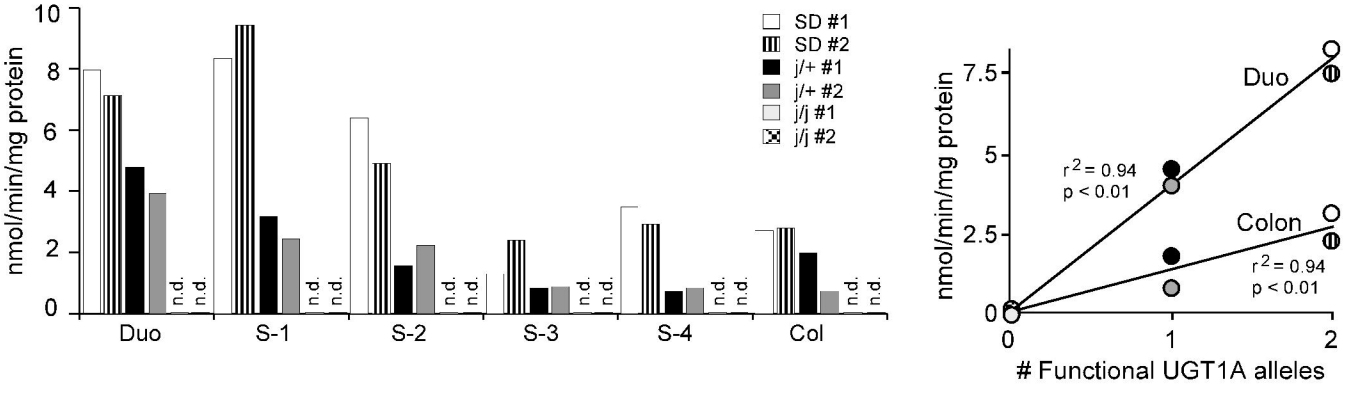

Figure 6

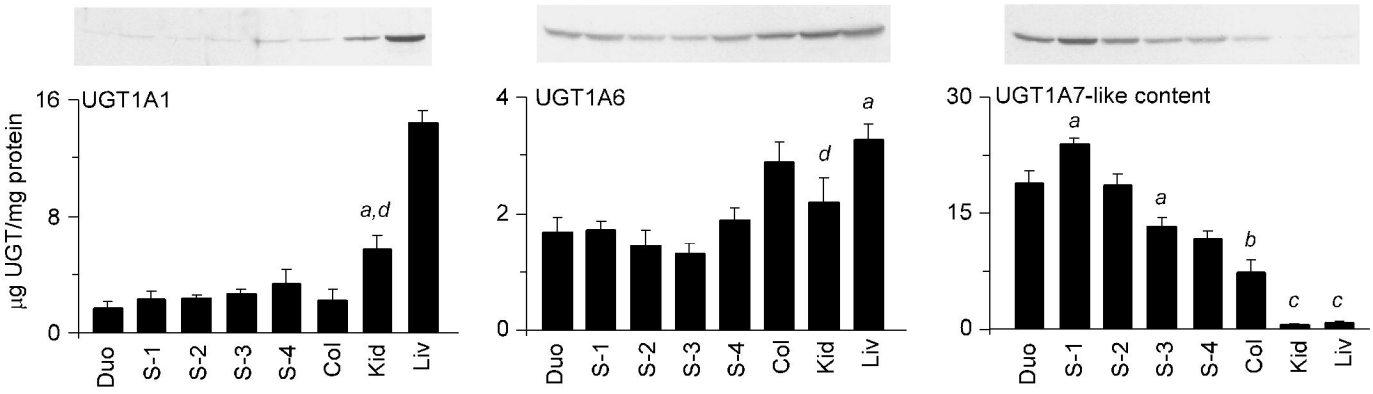
UGT1A1
UGT1A6
UGT1A7-like content
µg UGT/mg protein
16
8
0
4
2
30
15
a,d
a
d
a
b
c
c
Duo
S-1
S-2
S-3
S-4
Col
Kid
Liv

DMD Fast Forward. Published on June 21, 2006 as DOI: 10.1124/dmd.106.010140
This article has not been copyedited and formatted. The final version may differ from this version.

Figure 7